

Stabilization Study of Modified PAN- co-Polymer Composite Nanofibers with Functionalized Single-Walled Carbon Nanotubes

Fateme Farhadi; Marjan Abbasi*, Akbar Khodaparast Haghi

*Department of Textile Engineering, Faculty of Engineering, University of Guilan, Rasht, Iran; Email: m.abbasi@guilan.ac.ir; P.O.BOX 41635-3756

Abstract

In the present study, polyacrylonitrile (PAN)-co-polymer nanofibers as well as PAN-co-polymer nanofibers reinforced with functionalized single-walled carbon nanotubes (F-SWCNTs) were produced by electrospinning and stabilized. The samples were evaluated using DSC, FTIR, SEM and XRD.

In the sample containing F-SWCNT the amount of heat released during the stabilization reactions was lower than that of pure PAN nanofibers. This indicates that the F-SWCNT prevents the sudden release of heat and damage to the nanofibers during stabilization. The carbon nanotubes greatly prevent the reduction of the diameter of the nanofibers as well as the decrease in the size of the crystals and the decrease of the arrangement of the nanofibers during stabilization.

Key words: Stabilization; Co-Polyacrylonitrile; Single-walled carbon nanotube; Nanofibers

1- Introduction

Carbon nanotubes (CNTs) are hollow cylindrical structures that are divided into two types of single-walled nanotubes (SWCNT) and multi-walled nanotubes (MWCNT). These materials have been widely used as additives to modify the properties of different polymers and to produce composites [1-4].

These materials have unique mechanical, thermal and optical properties and are used as reinforcers in composite nanofibers [5-6]. The addition of these materials alters the viscosity and electrical conductivity of the polymer solution and can also affect the microstructural properties and the crystallinity of the nanofibers [5].

CNTs tend to accumulate in the form of clusters due to their high length to diameter ratio, large specific surface area, high flexibility, electrostatic interaction and the presence of Vander Waals forces [7]. Different methods are used to treat CNT accumulation. Physical methods use surface-active materials [8]. Chemical methods also include the surface modification or functionalization with various chemical groups such as hydroxyl (OH) or carboxylic acid (-COOH) to disperse CNTs in a liquid media and increase the resistance to accumulation [9].

The presence of functional groups in CNTs can increase their reactivity and interaction with the polymer substrate. The polymer wrapping process is achieved through the Vander Waals interactions and chemical bonding (π - π stacking) between CNTs and polymer chains containing aromatic rings [10]. However, Functionalizing is not a reason for the interaction [9, 11].

In recent years, polyacrylonitrile (PAN) / CNT composites have attracted much attention. The PAN is an important polymer that interacts well with the CNT. The thermal stability of polymers may also be altered by the presence of nanotubes, which is associated with crystallinity and mobility of polymer chains, making composites susceptible to application at high temperatures. It has been observed that by adding CNT to the polymer substrate, the glass transition temperature (T_g) as well as the thermal expansion and diffusion coefficient of the

composites increase at temperatures above T_g. Increasing these parameters allows composites to be used as coatings because the higher T_g temperature increases the composite fluidity and creates a more uniform flow of materials through the nozzle [12]. As the arrangement of CNTs increases, the molecular arrangement of PANs also increases. In the presence of CNTs irregularly embedded in the polymer, the improvement of the polymer / CNT composite properties is limited [12, 13]. These composites are prepared with solvents such as dimethylformamide, dimethylacetamide or dimethylsulfoxide by various spinning methods such as: conventional spinning, gel spinning and electrospinning [12, 14, and 15].

Since PAN-containing composite fibers used to produce carbon fibers have to be heat treated, and on the other hand, the diameter of the primary fibers has a great influence on the properties of the final carbon fibers, so the diameter of the primary fibers and the spinning method are of great importance. The lower diameter of the nanofibers produced by electrospinning improves them compared to the fibers produced by solution spinning methods. This causes the number of the binding sites of nanofibers to increase, thus it can improve the mechanical properties and electrical conductivity of the nanofibers. If the diameter of the primary fibers is reduced to the nanoscale, the core-shell structure of the final carbon fibers is dramatically reduced and the heat transfer improves and, during stabilization, the heat flows uniformly throughout the fiber. According to the above, the best method for preparing PAN/CNT composite nanofibers is electrospinning [16]. In the electrospinning, the polymer solution is removed from the spinneret as the solvent evaporates under the electrostatic field and a nonwoven layer is collected on a metal collector [5]. The electrospun nanofibers are used today in a variety of fields; for example, hydrogen storage, fuel cell, tissue engineering, drug release systems, environmental engineering, defense industries, nanocomposites and filtering [17-20].

The effect of comonomers on the thermal behavior of PAN has been investigated by many researchers. Comonomers and their selection have a significant impact on the stabilization process by interfering with the nitrile-nitrile interactions to increase the mobility of polymer chain segments [21-22]. There are basically three ways to perform heat treatment during the stabilization of the fibers: isothermal stabilization, stabilization by stepwise stabilization temperature, and single-phase stabilization [23].

The main objective of this study is to investigate the modified properties of PAN co-polymer with single-walled carbon nanotube (SWCNT). In the present study, PAN co-polymer nano fibers (with methyl methacrylate comonomer) and PAN co-polymer nano fibers reinforced with single-walled carbon nanotube functionalized (F-SWCNT) with carboxylic acid were prepared by electrospinning and then stabilized. The product characteristics were evaluated by XRD, DSC, FTIR, and SEM.

2- Experimental

2-1 Materials

PAN-co-polymer containing 94.6% acrylonitrile monomer and 5.4% methyl acrylate monomer with molecular weight of 100000 g/mol produced by Isfahan's Polyacryl Company was used. The F-SWCNT was prepared from Nuterino (with a diameter of 1-2 nm, 30 μ m length, 90% purity and 2.73% weight COOH) and 380 g/m² specific surface area. The N, N-dimethylformamide (DMF) solvent with purity greater than 99% was used as the PAN solvent prepared by Merck Company.

2-2 Equipment

2-2-1 Viscometer & Electrical conductivity meter

For the evaluation of the viscosity and electrical conductivity of solutions, a rotary viscometer (Brookfield, DV-II+Pro) and a conductivity meter (Model DDS-307, China) were employed.

2-2-2 Ultrasonic Probe

The Ultrasonic Probe model HD 3100 with working power of 50 W was used to disperse F-SWCNT in a DMF solvent. The probe used is an acid type that must be immersed in the solution to a height of 3 cm.

2-2-3 Electrospinning Device

The Japanese N1235 Syringe Pump was used to produce the nanofibers, and the voltage was supplied by Gamma high voltage. The 2ml syringe and the G22 needle (needle length 34 mm and needle inner diameter 0.4 mm and outer diameter 0.7 mm) were used for electrospinning.

2-2-4 Polarized Light Microscope

The Japanese FXL / FXA Polarized Light Microscope was used to determine the optimum conditions for electrospinning and the observation of the electrospined nanofibers.

2-2-5 Scanning Electron Microscope (SEM)

The morphologies of the composite scaffolds were observed using a scanning electron microscope (SEM) (EM3200/ KYKY/20kV) after a conductive layer coating (SBC12-Sputter coater) with a fixed collector. The device was used to observe the structure of nanofibers and measure their diameter.

Image J software was used to measure the diameter of nanofibers. For this purpose, the diameters of 100 different points of the fibers were measured and the mean (d), standard deviation (STD) and coefficient of variation (CV %) were calculated. Statistical analysis of variance (ANOVA) and Scheffe test were performed at the confidence level of 95% by means of SPSS 17 software.

2-2-6 Fourier Transform Infrared Spectroscopy (FTIR)

The FTIR spectroscopy is used to investigate the chemical structure and functional groups. The device used is Nicolet Magna Model 560 IR made in USA. To investigate the structure of PAN/F-SWCNT nanofibers after electrospinning as well as the structure of nanofibers at different stabilization temperatures, spectroscopy was performed in the range of 400-4000 cm^{-1} wavelength. To analyze the results of FTIR, E.S.P OMNIC Nicolet software was used.

2-2-7 X-ray diffraction (XRD)

The crystallinity and size of the crystals in nanofibers were investigated by Philips X-ray diffraction (XRD) model PW1840/01. A diffractometer with Ni filtered $\text{CuK}\alpha$ radiation ($\lambda = 1.5418\text{\AA}$, is the wavelength of the incident X-ray beam) at 40 kv and 30 mA was used to

obtain the XRD pattern of nanofibers. To calculate the distances between planes, the Miller Index, (*hkl*), Bragg's equation was used in accordance with Equation 1 [24].

$$d_{hkl} = \frac{\lambda}{2 \sin(\theta)} \quad (\text{Equation 1})$$

Where d_{hkl} is the distance of the planes with the Miller Index (*hkl*), λ is the X-ray wavelength, $\lambda=1.5418^\circ\text{A}$ and θ is the diffraction angle.

Scherrer method was used to calculate the crystal size according to Equation 2 [24].

$$L_c = \frac{0.9 \lambda}{\beta \cos(\theta)} \quad (\text{Equation 2})$$

Where L_c is the crystal size and β represents full width at half maximum height. Crystallinity can be calculated from the ratio of the integrated area of all crystalline peaks to the total integrated area under the XRD peaks. The crystallinity of the samples (X_c) was calculated according to Equation 3 [21].

$$X_c = \frac{I_c}{I_a + I_c} \times 100 \quad (\text{Equation 3})$$

Where, I_a and I_c are the integrated intensities corresponding to the amorphous and crystalline phases, respectively

2-2-8 Differential Scanning Calorimetry (DSC)

The DSC-60 (company "Shimadzu," Japan) was used for thermal analysis of the samples. Thermal analysis was performed in the temperature range of 40-400 °C in air atmosphere with an increase in temperature of 10 °C/ min for PAN and PAN/ F-SWCNT nanofibers.

2-2-9 Electric Furnace

The electric furnace manufactured by Nabertherm Controller was used to stabilize PAN and PAN/F-SWCNT samples. The rate of increase in temperature of 1°C/min was used for stabilization.

2-3 Method of Testing

2-3-1 Preparation of PAN/FSWCN composite nanofibers

The optimized electrospinning conditions of the PAN solution were determined at a concentration of 12(w/v %). Another factor that influences the choice of concentration is the diameter of the nanofibers. For nanofibers to be able to withstand high temperatures during heat treatment, they must have a diameter greater than 300 nm. According to these two factors (fiber-free bead and proper diameter) a suitable concentration of 12% was determined. Feeding rate: 2 µl/ min, voltage: 8 kv and spinning to collector distance: 18 cm. Functionalized nanotubes with COOH group were used for proper dispersion of carbon nanotubes in a DMF solvent. An ultrasonic device is used to disperse nanotubes. According to studies and experiments, the best time for sanitization was 15 minutes. However, if the

operation time is long, CNTs will be damaged and shortened and their desired properties will be reduced [25].

2-3-2 Method of heat treatment

Samples were electrospun on an aluminum foil collector for 20 h to reach an acceptable thickness. The web nanofibers containing 0, 0.5, 1 and 2wt% F-SWCNT was produced (this was calculated in relation to the dry polymer mass), but in samples containing 2% F-SWCNT, a small amount of incompatibility after stabilization was observed in the diameter of nanofibers; this can be attributed to the high percentage of carbon nanotubes. Also the 0.5% F-SWCNT of nanotubes had no appreciable effect on the thermal behavior of the polymer.

According to previous works on the stabilization of PAN, structural changes began slowly at 180° C and continued until the temperature of 270° C. At temperatures above 270° C due to excessive oxygen uptake, oxidation occurs which is not desirable. Therefore, the temperature range of 180-270° C was found to be suitable for stabilization. Since the PAN and PAN/F-SWCNT samples are compared together in the stabilization phase, a uniform temperature range was used to stabilize all the samples. From the above temperature range, 180° C, 230° C and 270° C were selected for stabilization. The rate of temperature increase is one of the most important factors in the stabilization phase. Most researchers who have studied the stabilization of PAN have reported the best stabilization with an increase in temperature of 1 °C/min. Samples stabilized at high rate of increase in temperature have a brittle and non uniform appearance that are not suitable for the subsequent transfer [23] and remain at that temperature for up to 1 hour after reaching the desired temperature.

3- Results and Discussion

3-1 Dispersion study of F-SWCNT

As mentioned before, the ultrasonic probe was used to disperse carbon nanotubes in a DMF solvent. To investigate the dispersion stability of carbon nanotubes for the production of composite nanofibers, solutions containing 0 wt% (F-SWCNT-0) and 1 wt% (F-SWCNT-1) of F-SWCNT were checked out for one month. After one month, no F-SWCNT residue was observed, and the solutions were completely stable. The dispersion of CNTs in polymer solutions, due to their high length-to-diameter ratio, large specific surface area, high flexibility, and the presence of Vander Waals and gravitational forces, can face many challenges, which can lead to their sediment [26]. By using carbon nanotubes functionalized with carboxylic acid groups, a stable dispersion in the desired solvent can be achieved by repulsion between the -COOH groups.

3-2 Morphology of the electrospun nanofibers

Since The optimized electrospinning conditions of the PAN solution were determined at a concentration of 12(w/v %) and increasing the amount of carbon nanotubes to polymeric solution increases the electrical conductivity of the polymer solution (the electrical conductivity values of PAN and F-SWCNT-1 are 0.38 ± 0.02 and 2.53 ± 0.05 $\mu\text{S/cm}$ respectively) resulting in a larger electric current during the electrospinning process in the fluid jet; Therefore, with increasing the load accumulation, the adhesion forces will be overcome and the repulsive forces of the accumulated loads between the nanofibers will be intensified and as a result the velocity of the electrospinning process can be increased, and therefore the fluid jet does not

have enough time to be optimally elongated by bending instabilities, As a result, the diameter of the nanofibers increases significantly by adding the carbon nanotubes in solution [27, 28]. On the other hand, the carbon nanotubes can increase the viscosity of the polymer solution (in samples PAN and F-SWCNT-1 the viscosity values are 419.9 ± 11.4 and 467.5 ± 14.2 cP, respectively) and thus increase the viscoelastic force in the electrospinning process and increase the diameter of the nanofibers [29-31]. Figure 1 shows that with the addition of F-SWCNT to the solution, the diameter of the nanofibers increased. The results of ANOVA and Scheffe test show that the increase of FSWCN at all levels caused a significant change in the diameter of nanofibers at the confidence level of 95%.

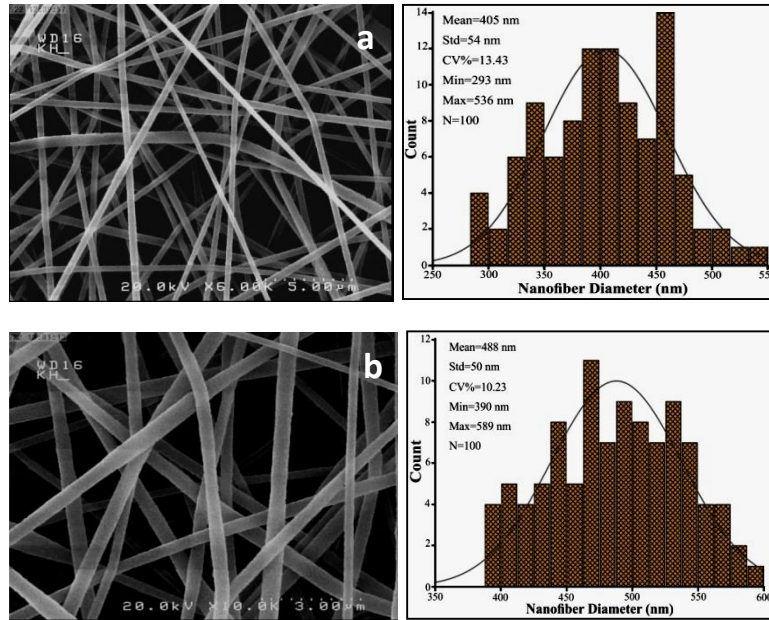


Figure 1 - SEM images of the (a): PAN and (b): F-SWCNT - 1 nanofibers and the diameter distribution

3-3 Investigation of thermal behavior of nanofibers

The exothermic peak of PAN has been reported to be varying between 200 and 350 °C depending on the cyclization, dehydrogenation, and oxidative reactions. The exothermic peak of PAN electrospun nanofibers is due to the cyclization reactions which can take place at high temperature, leading to the consumption of a small part of nitrile groups[32].

Figure 2 shows the DSC diagrams of samples of nanofibers produced in the air environment. The values of initial temperature (T_i), final temperature (T_f), peak temperature (T_{pk}), peak width (ΔT) and released heat (ΔH) of these samples are given in Table 1. It should be noted that the DSC diagrams of these nanofibers were obtained at a rate of increase of 10°C/min.

In the F-SWCNT-1, the initial temperature (T_i) and peak temperature (T_{kp}) are shifted to higher temperatures than pure PAN nanofibers. The initial temperature in the pure PAN nanofibers is 294.8, with the addition 1 wt % F-SWCNT; the initial temperature reached 299.7 °C. Since the polymer concentration is the same in two samples (12 w/v %), so the changes in the morphology of the nanofibers can be related to its carbon content. This variation might be

due to changes in crystallinity or to varied ratios of crystalline to amorphous domains across the fibers with the addition of FSWCNT.

The DSC results are important because they may detect the range of operating temperatures in which the nano-fiber are used and results correlate well with the ultimate thermo-mechanical stability and physical strength of the nanofiber. The stabilization stage involves several complex reactions that take place in an oxygen-containing environment. The oxygen penetration in the amorphous regions is much easier and faster than the crystalline regions, thus stabilizing reactions start from the amorphous regions and then penetrate into the crystalline regions; on the other hand, addition of CNT reduces the mobility of polymer chains and increases its hardness compared to PAN fibers; as a result, oxygen penetration in these areas is slow and difficult, and the onset of stabilization reactions is delayed, and consequently the temperature of the onset of the exothermic reaction is shifted to higher temperatures [33]. The amount of heat released in the presence of F-SWCNT (2.34 J) decreased compared to pure PAN (4.21 J). The heat released during the stabilization reactions is influenced by two factors: the first type of reaction and the second the rate of reaction progress. Oxidation releases the highest amount of heat of the stabilization reactions; therefore, the exothermic peak in the DSC diagram of nanofibers is mostly related to the oxidation reaction during stabilization [33].

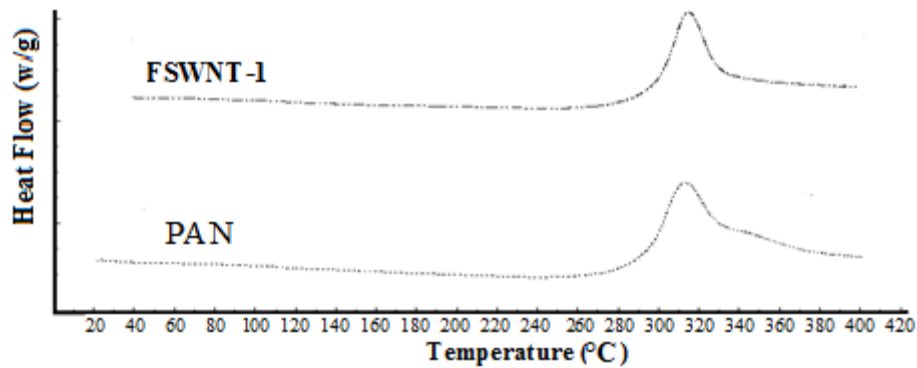


Figure 2 - the DSC diagram of composite nanofibers with F-SWCNT and PAN

Table 1- Thermal properties of DSC diagram of PAN and F-SWCNT-1 composite nanofibers

Sample	Initial Temperature T_i (° C)	final Temperature T_f (° C)	peak Temperature T_{pk} (° C)	$\Delta T = T_f - T_i$ (° C)	ΔH (J)
PAN	294.8	333.7	313.1	38.9	4.21
F-SWCNT-1	299.7	329.9	315	30.2	2.34

One of the factors that influence the rate of reaction progression is the diameter of nanofibers. The previous section showed that the diameter of PAN nanofibers increased with the addition of F-SWCNT. In the nanofibers with F-SWCNT, due to the need for longer time, the oxidation reaction may not be complete, resulting in less heat release; in general, it can be said that by adding F-SWCNT, the exothermic reactions during stabilization are performed in milder

conditions, thereby releasing less heat. As a result, defective areas in the structure of the final carbon fiber are prevented [33].

Accompanied by the temperature shifts, the broadness of the peak decrease in F-SWCNT-1 sample. It is well known that the first exothermic peak is attributed as the cyclization reaction of PAN molecules. The shifted and broadened peak patterns show that the exothermic cyclization reaction of PAN was facilitated and reduced when the fibers were accompanied with F-SWCNT.

3-4 the investigation of the morphology and diameter of nanofibers after stabilization operation

Figure 3 shows the SEM images of PAN nanofibers and F-SWCNT-1 stabilized at 270° C along with the diameter distribution. The images show that the structure of nanofibers in samples was perfectly uniform.

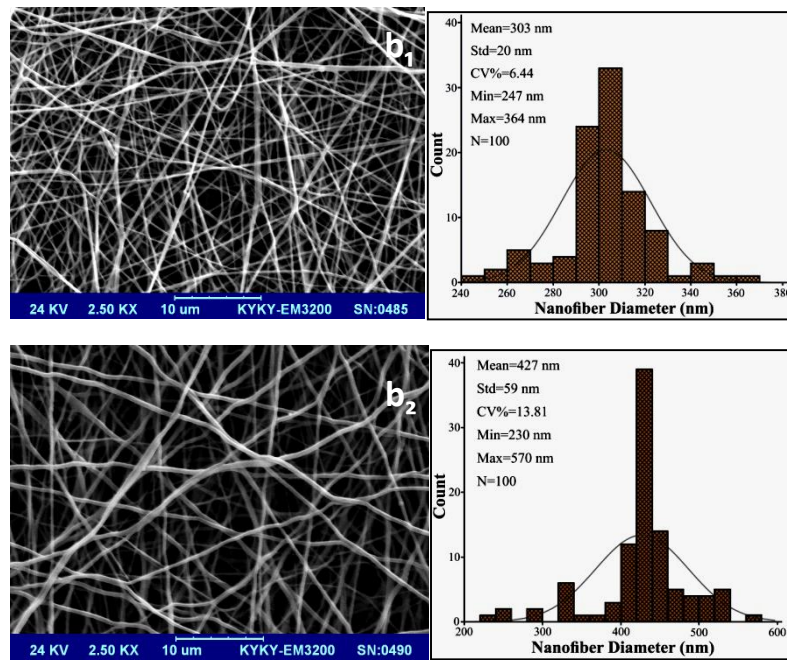


Figure 3 - SEM images of the stabilized (b_1): PAN; (b_2): (F-SWCNT - 1) and diameter distribution of nanofibers

As can be seen, during the stabilization, the diameter of pure PAN nanofibers reached from 405 ± 54 to 303 ± 20 (equivalent to 25% reduction), whereas in the F-SWCNT-1, the diameter decreased from 488 ± 50 to 427 ± 59 (equivalent to 12.5% reduction). It can be said that the presence of F-SWCNT prevented the reduction of nanofibers diameter during stabilization.

By applying thermal stabilization operations, the fibers tend to be released from the initial stresses. This release of stress causes the fibers to shrink. With the addition of F-SWCNT, the crystallinity is increased, thereby making the polymer chains unable to move easily. It makes the carbon nanotubes resistant to tensile stress. And as a result, they do not change easily; carbon nanotubes can also prevent thermal shrinkage of the fibers. The DSC results revealed that the addition of F-SWCNT caused stabilization reactions to be performed in milder conditions and less heat is released. Reaction at milder conditions means that the nanofibers are

not exposed to sudden heat release and, as a result of heat treatment, their structure changes less [33].

3-5 The investigation of chemical structure changes of nanofibers during stabilization

The FTIR spectra of nanofibers, heat treated at three different temperatures are shown in Figures 4 and 5. According to FTIR results, several chemical reactions occur during stabilization as follows:

The reaction of nitrile groups ($\text{N} \equiv \text{C}$) resulting in a structure containing the $\text{N} = \text{C}$ group. This group is formed as a result of intermolecular cyclization or the formation of intracellular crosslinks. The structural formation of the $\text{C} = \text{C}$ group results from the dehydrogenation. Oxidation gives rise to carbonyl groups ($\text{O} = \text{C}$). The index peak in the PAN fibers structure belongs to the nitrile group ($\text{N} \equiv \text{C}$) with a wave number of 2243 cm^{-1} , which showed the most change during the heat treatment and decreases with increasing temperature. As the height of peak decreases to a 2243 cm^{-1} , a new peak is generated at a 1595 cm^{-1} corresponding to a combination of $\text{H} - \text{N}$, $\text{C} = \text{C}$, and $\text{N} = \text{C}$. During the stabilization, the peak of the $\text{N} \equiv \text{C}$ group does not completely disappear, confirming that a number of $\text{N} \equiv \text{C}$ groups remains in the fiber structure, indicating a stable semi-circular fibers structure [34, 35].

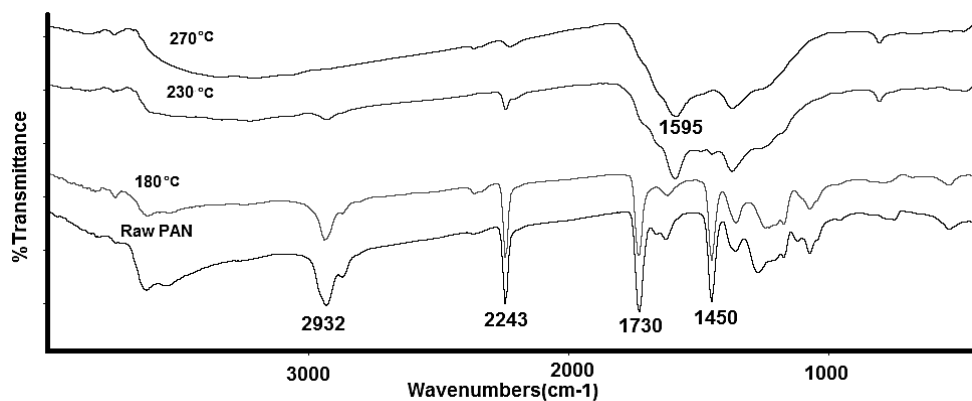


Figure 4- FTIR spectra of raw PAN and stabilized PAN nanofibers at different temperatures

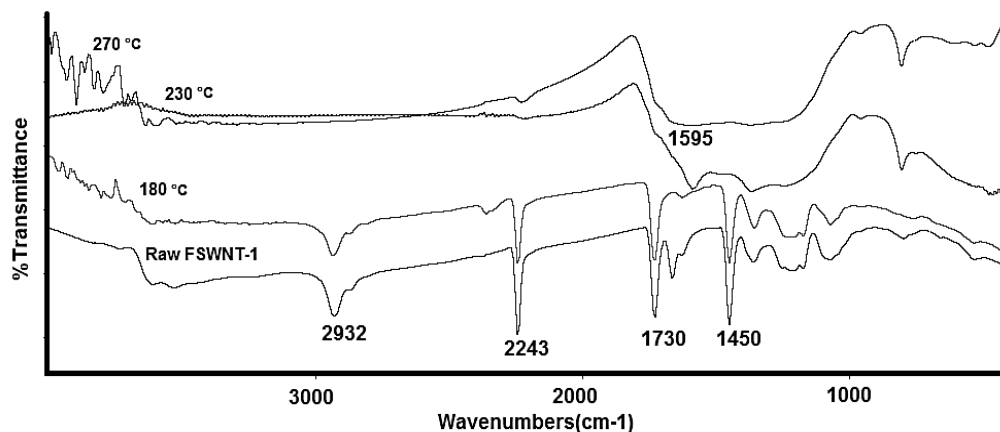


Figure 5- FTIR spectra of raw and stabilized F-SWCNT-1 nanofibers at different temperatures

The FTIR results of the nanofibers produced show that the stabilization reactions are poorly initiated at 180 °C. As the temperature increases, the peak height of the nitrile group decreases to a wave number of 2243 cm⁻¹ and a 1730 cm⁻¹ corresponding to the ester O=C groups in the fibers. The presence of the nitrile group peak is also observed at the highest temperature (270 °C); indeed, if all nitrile groups undergo a cyclic reaction, the N ≡ C peak must be completely eliminated, but since a cyclic reaction occurs randomly and some of the nitrile groups are isolated and hard to react with, therefore, small amounts of nitrile groups always remain in the structure of fibers after stabilization, thereby resulting in the formation of semi-circular structures in the stabilized nanofibers.

As the stabilization temperature increases, the peak heights in 1450 cm⁻¹ and 2932 cm⁻¹ corresponding to the aliphatic methylene group in the linear structure decrease, and a new, broader peak at 1595 cm⁻¹ is created, which pertains to the C=C and N=C groups in the stable nano-fiber structure; also with the stabilization progress, a new peak in the 810 cm⁻¹ corresponding to the H-C = C group is created in the nano-fiber structure. The removal of the peaks of the aliphatic methylene group and the emergence of new peaks in the 1595 cm⁻¹ and 810 cm⁻¹ emphasize the conversion of linear structure to semi-cyclic structure with the progress of the cyclization and dehydrogenation reactions during stabilization [36].

The peak position corresponds to the nitrile group in the raw nanofibers at a wave number of 2243 cm⁻¹. At 180 °C, the peak position remained unchanged but its height decreased. This indicates that the number of primary nitrile groups (non-reactive nitriles) decreased to a small extent. With the increase in temperature, not only the decrease in peak height, but also its position has also changed. At a temperature of 230 °C, the nitrile group peak has more broad range and less height, and at a temperature of 270 °C the peak position changed and moved to a lower wave number. It can be justified that, with the onset of stabilization reactions, the primary nitrile groups enter the cyclic reaction and their amount decreases. At higher temperatures and with the progress of the stabilization reactions, some of these primary nitrile groups, as the reactions occur, are converted to conjugated nitrile and β-amino nitrile groups. So that at high stabilization temperatures, the peaks of these two groups of nitriles are formed, and since the peaks of these three types of nitrile groups are very close together, the formation of the other two peaks causes the initial peak to increase. Finally, increasing the number of β-aminonitrile groups causes the peak position shift to a lower wave number.

According to the FTIR spectra, the increase of the peak of the nitrile group at 230 °C and the change of position of the peak at 270 °C in the pure PAN nanofibers is greater than that of the composite nanofibers. This indicates that the formation of β-amino nitrile groups decreased in the presence of F-SWCNT. As a result, stabilized F-SWCNT-1 nanofibers will have better properties than pure PAN nanofibers.

The Extent of Reaction (*EOR*) was used to investigate the impact of F-SWCNT on the progress of stabilization reactions. This index was calculated by Equation 4 [37]. The results of this calculation for nanofibers produced at different stabilization temperatures are presented in Table 2.

$$EOR = \frac{I_{2243}}{I_{1595} + I_{2243}} \quad (\text{Equation 4})$$

In this Equation, I_{2243} is the peak intensity at the 2243 cm⁻¹ and I_{1595} is the peak intensity at the 1595 cm⁻¹. The *EOR* value varies between 1 and 2.

Table 2- Extent of Reaction (EOR) values for stabilized PAN and composite nanofibers

Stabilization Temperature(°C)	EOR	
	PAN	F-SWCNT-1
180	0.097	0.059
230	0.881	0.816
270	0.954	0.958

According to the results of the table 2, at 180 °C the stabilization reactions for pure PAN nanofibers is higher than that of F-SWCNT-1 sample, indicating that at low temperatures (180 °C) the progress of stabilization reactions in the presence of F-SWCNT is delayed and reduces the amount of stabilization index.

As the amorphous regions in pure PAN nanofibers is higher than that of F-SWCNT-1 sample therefore stabilization reactions in pure PAN due to access to more amorphous regions start earlier and progress further [33]. At the temperature of 230° C, the EOR of pure PAN sample is also higher than that F-SWCNT, but at 270 °C two samples have almost equal EOR. It appears that at low temperatures due to the complete inactivation of the stabilizing exothermic reactions, there is no energy required to penetrate the crystalline regions, but as the temperature rises and the initiation of exothermic reactions, the energy required to penetrate the crystalline regions is generated by heat provided, and stabilization reactions penetrate the crystalline regions. As a consequence, at high temperatures, stabilization is performed to the same extent throughout the nanofibers structure.

3-6 investigation of crystal structure changes of nanofibers after XRD stabilization

The crystal structure of the pure PAN sample and F-SWCNT-1 were compared. The XRD spectra and the properties of the raw and stabilized nanofibers spectra at 270°C are shown in Figures 6 and 7 and table 3, respectively. As can be seen from the figures, the intensity of peak $2\theta = 17$ decreased after stabilization at 270 °C, and a new peak was created at $2\theta = 25$ instead. The appearance of this broad peak in the XRD spectrum indicates the onset of graphite crystal structure growth and the conversion of linear structure to cyclic structure during heat treatment [33, 38].

The values in the table 3 shows that with stabilization at 270 °C, the peak center of the plane (100) did not change much, but the height and area under the peak decreased significantly. The decrease in height and area under the peak of the plane (100) in the sample containing 1 wt% F-SWCNT is greater than in the pure PAN sample. This decrease affects the crystallinity of the stabilized nanofibers. As can be seen, during the stabilization, the crystallinity of pure PAN nanofibers reached from 44% to 38% (equivalent to 6.13% reduction), whereas in the sample containing 1 wt% F-SWCNT, the crystallinity decreased from 47% to 24% (equivalent to 9.48% reduction).

Therefore, during stabilization, the crystallinity of the nanofibers decreased and this decrease in crystallinity is greater in F-SWCNT-1 sample. The size of the crystals also decreased due to heat treatment during stabilization, indicating that with high temperatures, the crystalline regions are also involved in stabilizing reactions and consequently the size of the crystals decreases. As a result of heat treatment, the crystalline particle size in the pure PAN was reduced from 26.9 nm to 11.4 nm (equivalent to 57.5% reduction) and in F-SWCNT-1 sample, decreased from 18.3 nm to 11.84 nm (equivalent to 35.4% reduction). The DSC results

revealed that in the presence of F-SWCNT, the stabilization reactions proceeded slowly, and the reaction heat was not released abruptly, which caused the stabilization reactions to be performed in milder conditions. And also carbon nanotubes, like chambers around the crystals, prevent large changes in the crystal size during stabilization.

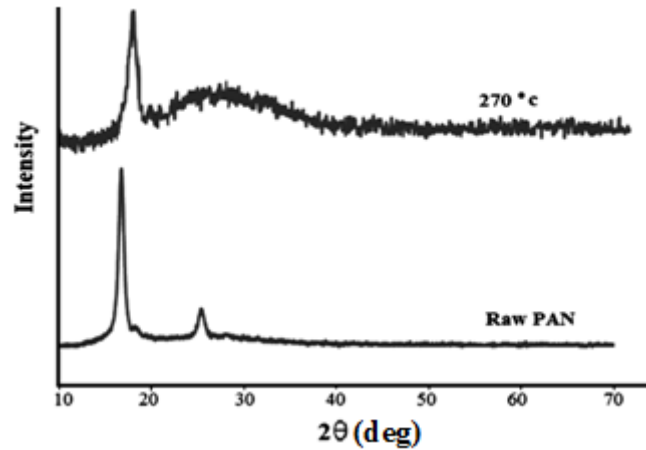


Figure 6 - XRD spectra of raw and stabilized PAN nanofibers at 270 ° C

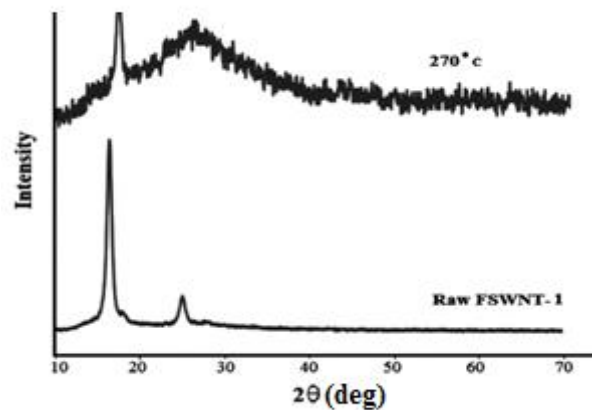


Figure 7 - XRD spectra of raw and stabilized F-SWCNT-1 nanofibers at 270 ° C

Table 3- Characteristics obtained from XRD results for raw and stabilized nanofibers at 270 °

Sample	2θ (degree)	d-spacing (Å)	Peak Height(A)	Peak Area	Crystal Size (nm)	L_c/d_{100}	Crystallinity (%)
PAN (raw)	16.7	5.3	2415	2719.8	26.9	50.6	44
PAN (Stabilized)	17.0	5.2	922	2087.6	11.4	22.1	38
F-SWCNT-1 (raw)	16.3	5.5	3845	4364.4	18.3	33.7	47
F-SWCNT-1 (Stabilized)	17.0	5.2	543	1773.3	11.8	22.8	24

According to Figures 6 and 7, the peak growth of $2\theta = 25$ is greater in the stabilized F-SWCNT-1, and is higher than in the stabilized pure PAN sample. This indicates that the crystal sizes of the cyclic structure (corresponding to the peak $2\theta = 25$) in F-SWCNT-1 are a little larger. In fact, carbon nanotubes are embedded in the PAN polymer substrate, thereby facilitating the growth of the crystals of the cyclic structure during stabilization [14].

The calculation of L_c/d_{100} values for the two stabilized pure PAN and F-SWCNT-1 indicated that the arrangement decreased with stabilization in both samples, And decreasing the arrangement in the pure PAN sample (from 50.63 to 22.07) is more than F-SWCNT-1 sample (from 33.65 to 22.77); in fact, the presence of carbon nanotubes preserves the arrangement during heat treatment.

During thermal stabilization, the peak intensity of $2\theta = 17$ decreased markedly, and this peak did not interfere with other peaks; Therefore, by using the intensity of this peak in raw fibers and stabilized fibers, the stabilization index (SI) can be calculated at 270°C . The stabilization index is used to quantify the progress of PAN fiber stabilization operations, obtained by the Equation 5 [39].

$$SI = \left(\frac{I_o - I}{I_o} \right) \quad (\text{Equation 5})$$

I_o is the peak diffraction intensity of $2\theta = 17$ in raw PAN fiber and I is the peak diffraction intensity of $2\theta = 17$ in the stabilized PAN fiber. Also, the aromaticity index (AI) of the samples was calculated by Equation 6. This index is used to evaluate the degree of cyclic structure formation in fibers [40]. The results of these calculations are presented in Table 4.

$$AI = \left(\frac{I_{25}}{I_{25} + I_{17}} \right) \quad (\text{Equation 6})$$

In this Equation, I_{25} and I_{17} are the diffraction intensities of $2\theta = 25$ and $2\theta = 17$, respectively.

Table 4- Aromaticity Index (AI) and Stabilizing Index (SI) values of PAN and F-SWCNT-1 nanofibers stabilized at 270°C

Sample	AI	SI
PAN	0.24	0.62
F-SWCNT-1	0.36	0.86

As shown in Table 4, for the F-SWCNT-1 sample the values of both stabilization and aromaticity indices were higher than for pure PAN samples. Since the crystallinity in the sample containing carbon nanotubes is higher than that of pure polymer, therefore, at high temperatures the sample containing carbon nanotubes exhibits greater improvement in stabilization, and therefore the stabilization and aromaticity indicated for the sample containing F-SWCNT are greater.

4- Conclusion

The PAN-co-polymer nanofibers and PAN-co-polymer nanofibers with F-SWCNT were produced by electrospinning and stabilized. The results showed that the nanofibers were produced uniformly without structural defects. With the addition of F-SWCNT the average diameter of the nanofibers increased.

The SEM images of stabilized samples at 270 ° C showed that the stabilization operation reduced the diameter of nanofibers, and this decrease was less in sample containing F-SWCNT. The addition of F-SWCNT to the PAN enhanced their thermal stability, thereby prevented their drastic structural changes during stabilization.

The FTIR spectra of the stabilized nanofibers at 270 °C showed that the formation of β -amino nitrile groups decreased in the presence of F-SWCNT. The lower the number of these groups in the fiber structure, the less the chains can be disrupted in the stabilized fibers, thereby resulting in less defective carbon fibers and better mechanical properties.

The XRD of the stabilized samples showed that in the sample containing F-SWCNT, the values of both stabilization index and aromaticity index were higher than those of pure PAN sample. In other words, the improvement of stabilization reactions at 270 ° C in the presence of F-SWCNT is higher than pure PAN, and the presence F-SWCNT largely prevented the crystal size and the nanofibers arrangement decreasing during stabilization.

The DSC results showed that in the presence of F-SWCNT the starting temperature of the reaction and peak temperature shifted to higher temperatures. In fact, the presence of F-SWCNT delayed the onset of stabilization reactions at low temperatures, as well as in the sample containing F-SWCNT the amount of heat released during stabilization reactions was less than the pure PAN samples; this indicates that F-SWCNT causes stabilization reactions to be performed in milder conditions, and the sudden release of much heat did not occur in these samples. As a result, nanofibers do not become damaged during stabilization.

Acknowledgments

The work was supported by University of Guilan, Rasht, Iran.

References:

1. P-Ch. Ma, N. A. Siddiqui , G. Marom and J-K. Kim, Dispersion and functionalization of carbon nanotubes for polymer-based nanocomposites: A review, *Composites* 41 1345-1367 2010.
2. P. Heikkila and A. Harlin, Electrospinning of Polyacrylonitrile (PAN) Solution: Effect of Conductive Additive and Filler on the Process, *Polymer Letters* 3 437-445 2009.
3. J. Jiang, C.M. Xu, Y. Su, Q. Guo, F. Liu, C. Deng and X.M. Yao, Influence of carbone nanotube coatings on carbon fiber by ultrasonically assisted electrophoretic deposition on its composite interfacial property. *Polymers* 2015, 8, 302-3012
4. Z.Q. Su, J.W. Ding and G. Wei, Electrospinning: A facial technique for fabricating polymeric nanofibers doped with carbon nanotubes and metallic nanoparticles for sencore applications. *RSC Adv*, 4, 52598-52610, 2014.
5. M.K. Pilehrood , P. Heikkila and A. Harlin, Preparation of Carbon Nanotube Embedded in Polyacrylonitrile (PAN) Nanofibre Composites by Electrospining Process, *AUTEX Res. J.*, **12**, 1-6, 2012.
6. M. Zhang and J. Li, Carbon Nanotube in Different Shapes, *Mater. Today*. **12**, 12-18, 2009.
7. P-C. Ma, N. A. Siddiqui, G. Marom, J-K. Kim, Dispersion and functionalization of carbon nanotubes for polymer-based nanocomposites: A review. *Composites Part A: Applied Science and Manufacturing*, 2010. 41(10): p. 1345-1367.
8. G. Salimbeygi, K. Nasouri, A.M. Shoushtari, R. Malek and F. Mazaheri, Fabrication of Polyvinyl Alcohol/Multi-Walled Carbon Nanotubes Composite Electrospun Nanofibres and their Application as Microwave Absorbing Material, *Micro Nano Lett.*, **8**, 555-559, 2013.

9. S. Zhang, J. Y. Wub, C.T. Tse, and J. Niu, Effective Dispersion of Multi-wall Carbon Nano-tubes in Hexadecane through Physiochemical Modification and Decrease of Supercooling, *Sol. Energ. Mater. Sol. Cell.*, **96**, 124-130, 1951-1959, 2012.
10. A. Benko, M. Nocuń, M. Gajewska, M. Błażewicz, Addition of carbon nanotubes to electrospun polyacrylonitrile as a way to obtain carbon nanofibers with desired properties. *Polymer Degradation and Stability*, 2019. 161: p. 260-276.
11. T.A. Huber, Polymer-carbon nanotube composites, Technical Memorandum, (2004).
12. S. Prilutsky, E. Zussman and Y. Cohen, The effect of embedded carbon nanotubes on the morphological evolution during the carbonization of poly (acrylonitrile) nanofibers, *Nanotechnology* 19, 2008.
13. T. Mikolajczyk, G. Szparaga, M. Bogun, A. Fraczek-Szczypta and S. Blazewicz, Effect of spinning conditions on the mechanical properties of polyacrylonitrile fibers modified with carbon nanotubes, *Journal of Applied Polymer Science* 115, 3628–3635, 2010.
14. H.G. Chae, Polyacrylonitrile /carbon nanotube composite fibers: Reinforcement efficiency and carbonization studies, PhD Thesis, School of Polymer, Textile, and Fiber Engineering, 2008.
15. S.M. Aqueel, Z. Wang, L. Than, G. Sreenivasulud and X.Q. Zeng, Poly (vinilidene fluoride)/poly (acrylonitrile)-Based superior hydrophobic piezoelectric solid derived by aligned carbon nanotubes in electrospinning: Fabrication, phase conversion and surface energy. *RSC Adv.*, 5, 76383-76391 2015.
16. Ch.K. Liu, K. Lai, W. Liu, M. Yao and R.J. Sun, Preparation of carbon nanofibres through electrospinning and thermal treatment, *Polym Int* 58, 1341–1349, 2009.
17. Z.M. Huang and Y.Z. Zhang, A Review on Polymer Nanofibers by Electrospinning and their Applications in Nanocomposites, *Compos. Sci. Technol.*, **6**, 2223-2253, 2003.
18. T. Jarusuwannapoom, T. Hongrojjanawiwat, S. Jitjaicham, L. Wannatong, M. Nithitanakul, C. Pattamaprom, P. Koombhongse, R. Rangkupan and P. Supaphol, Effect of Solvents on Electrospinnability Polystyrene Solutions and Morphological Appearance of Resulting Electrospun Polystyrene Fibers, *J. Eur. Polym.*, **41**, 409-421, 2005.
19. M. Rostamloo, M. Nouri M., and J. Mokhtari, Effect of Nanoclay on the Electrospinning of Poly (ϵ -caprolactone), *Iran. J. Polym.*, **24**, 3, 231-240, 2011.
20. G. Salimbeygi, K. Nasouri, and A.M. Shoushtari, Effect of Solution Concentration on Poly (vinyl alcohol) Nanofibers Structure, *J. New Mater.* **3**, 21-33, 2013.
21. D. He, Ch. Wang, Y. Bai, B. Zhu, Comparison of structure and properties among various PAN fibers for carbon fibers, *J. Mater. Sci. Technol.*, **21**, 2005.
22. P. Bajaj, T.V. Sreekumar and K. Sen, Thermal behavior of acrylonitrile copolymers having methacrylic and itaconic acid comonomers, *Polymer* 42, 1707–1718, 2001.
23. E. Fitzer, W. Frohs, M. Heine, Optimization of stabilization and carbonization treatment of PAN fibers and structural characterization of the resulting carbon fiber, *Carbon*, **24**, 387-395, 1986.
24. V. Anghelina, I.R. Popescu, A. Gaba, I.N. Popescu, R. Despa and D. Ungureanu, Structural analysis of PAN fiber by X-ray diffraction, *J. Sci. Art.* **10**, 89-94, (2010).
25. M. Wu, Q. Wang, K. Li, Y. Wu and H. Liu, Optimization of stabilization conditions for electrospun polyacrylonitrile nanofibers, *Polymer Degradation and Stability* 97, 1511-1519, 2012.
26. K. Nasouri, A.M. Shoushtari, A. Kafrou, H. Bahrambeygi and A. Rabbi, Single-Wall carbon nanotubes dispersion behavior and its effects on the morphological and mechanical properties of the electrospun nanofibers, *Polym. Compos.* **33**, 1951-1959, 2012.
27. S. Mazinani, A. Ajji and C. Dubois, Fundamental study of crystallization, orientation, and electrical conductivity of electrospun PET/carbon nanotube nanofibers, *Polym. Phys.* **48**, 2052-2064, 2010.
28. F. Farhadi, M. Abbasi, A. K. Haghi and K. Nasouri, Determination of morphological and microstructural properties of polyacrylonitrile/single-walled carbon nanotubes composite nanofibers, *Iranian Journal of Polymer Science and Technology*. **27**, 4, 267-279, 2014.
29. K. Saeed, S.Y. Park, Preparation and characterization of multi-walled carbon nanotubes/polyacrylonitrile nanofibers, *Polym. Res.* **17**, 535–540, 2010.
30. K. Saeed, S.Y. Park, H.J. Lee, J.B. Baek and W.S. Huh, Preparation of electrospun nanofibers of carbon nanotube/ polycaprolactone nanocomposite, *Polymer* 47, 8019-8025, 2006.
31. Y.J. Ryu, H.Y. Kim, K.H. Lee, H.C. Park and D.R. Lee, Transport properties of electrospun nylon 6 nonwoven mats, *Eur. Polym. J.* **39**, 1883-1889, 2003.

32. L. Jie, W. Lei and Z. Wang-Xi, *New Carbon Mater.* 20, 343, 2005.
33. Y.Liu, *Stabilization and Carbonization Studies of Polyacrylonitrile/ Carbon Nanotube Composite Fibers*, PhD Thesis, Georgia Institute of Technology, 2010.
34. Zh. Wangxi, L. Jie and W. Gang, Evolution of structure and properties of PAN precursors during their conversion to carbon fibers, *Carbon* 41, 2805–2812, 2003.
35. Q. Ouyang, L. Cheng, H. Wang and K. Li, Mechanism and kinetics of the stabilization reactions of itaconic acid-modified polyacrylonitrile, *Polymer Degradation and Stability* 93, 1415–1421, 2008.
36. M.M. Coleman and G.T. Sivy, Studies of the degradation of copolymers of acrylonitrile and acrylamide in air at 200°C, Speculation on the role of the peroxidation step in carbon fiber formation, *Carbon* 19, 123 (1981).
37. S. Dalton, F. Heatley and P.M. Budd, Thermal stabilization of polyacrylonitrile fibers, *Polymer* 40, 5531–5543, 1999.
38. Y.H. Choi, *Polyacrylonitrile/carbon nanotube composite fibers: Effect of various processing parameters on fiber structure and properties*, PhD Thesis, Georgia Institute of Technology, 2010.
39. M. Yu, Y. Bai, C. Wang, Y. Xu and P. Guo, A new method for the evaluation of stabilization index of polyacrylonitrile fibers, *Mater. Lett* 61, 2292–2294, 2007.
40. O.P. Bahl and L.M. Manocha, Characterization of oxidized PAN fibers, *Carbon* 12, 417–423, 1974.